mTORC2 Regulates Cardiac Response to Stress by Inhibiting MST1

Graphical Abstract
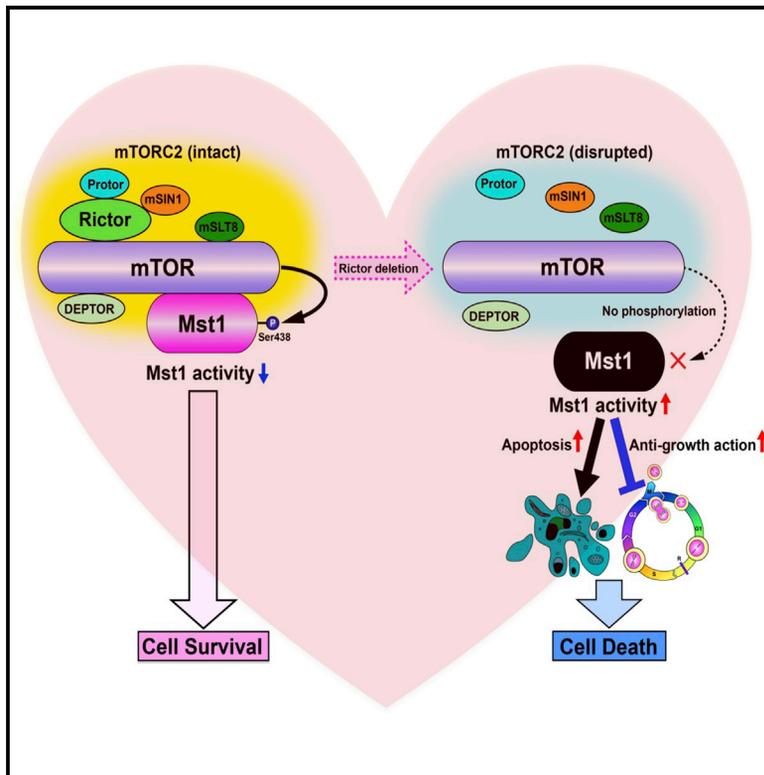
Authors

Sebastiano Sciarretta, Peiyong Zhai, ..., Hong Li, Junichi Sadoshima

Correspondence

sadoshju@njms.rutgers.edu

In Brief

The mTOR and Hippo pathways represent the major signaling pathways regulating cellular size and survival. Sciarretta et al. demonstrate the existence of a direct crosstalk between these two pathways. Rictor/mTORC2 preserves cardiac structure and function by phosphorylating MST1, a key component of the Hippo pathway, thereby restraining its activity.

Highlights

- mTORC2 preserves cardiac structure and function by restraining the activity of MST1

- mTORC2 phosphorylates MST1 at serine 438 in the SARAH domain

- MST1 phosphorylation by mTORC2 reduces its dimerization and activity

mTORC2 Regulates Cardiac Response
to Stress by Inhibiting MST1

Sebastiano Sciarretta,[1,2] Peiyong Zhai,[1] Yasuhiro Maejima,[1] Dominic P. Del Re,[1] Narayani Nagarajan,[1] Derek Yee,[1] Tong Liu,[3] Mark A. Magnuson,[4,5] Massimo Volpe,[2,6] Giacomo Frati,[2,7] Hong Li,[3] and Junichi Sadoshima[1,*]
[1]Cardiovascular Research Institute, Department of Cell Biology and Molecular Medicine, Rutgers New Jersey Medical School, Newark, NJ 07103, USA
[2]IRCCS Neuromed, Pozzilli 86077, Italy
[3]Center for Advanced Proteomics Research, Rutgers New Jersey Medical School, Newark, NJ 07103, USA
[4]Center for Stem Cell Biology, Vanderbilt University School of Medicine, Nashville, TN 37232, USA
[5]Department of Molecular Physiology and Biophysics, Vanderbilt University School of Medicine, Nashville, TN 37232, USA
[6]Division of Cardiology, Department of Clinical and Molecular Medicine, Faculty of Medicine and Psychology, Sapienza University of Rome, Rome 00187, Italy
[7]Department of Medico-Surgical Sciences and Biotechnologies, Sapienza University of Rome, Latina 04100, Italy
*Correspondence: sadoshju@njms.rutgers.edu
http://dx.doi.org/10.1016/j.celrep.2015.03.010

SUMMARY

The mTOR and Hippo pathways have recently emerged as the major signaling transduction cascades regulating organ size and cellular homeostasis. However, direct crosstalk between two pathways is yet to be determined. Here, we demonstrate that mTORC2 is a direct negative regulator of the MST1 kinase, a key component of the Hippo pathway. mTORC2 phosphorylates MST1 at serine 438 in the SARAH domain, thereby reducing its homodimerization and activity. We found that Rictor/mTORC2 preserves cardiac structure and function by restraining the activity of MST1 kinase. Cardiac-specific mTORC2 disruption through Rictor deletion leads to a marked activation of MST1 that, in turn, promotes cardiac dysfunction and dilation, impairing cardiac growth and adaptation in response to pressure overload. In conclusion, our study demonstrates the existence of a direct crosstalk between mTORC2 and MST1 that is critical for cardiac cell survival and growth.

INTRODUCTION

Cellular growth, proliferation, and survival are critical processes that must be finely regulated in order to preserve the structure and function of different organs. The mechanistic (previously called mammalian) target of rapamycin (mTOR) and Hippo pathways have recently emerged as the major signaling transduction cascades regulating organ size and cellular survival. The mTOR pathway promotes protein synthesis, cellular growth, and survival (Laplante and Sabatini, 2012; Wullschleger et al., 2006). On the other hand, the Hippo pathway exerts opposite effects, inhibiting cellular growth and proliferation and inducing cell death (Pan, 2010; Yu and Guan, 2013). This implies that tight

coordination of these two pathways is important for the regulation of organ size and cellular integrity, and it strongly suggests the existence of multiple crosstalk mechanisms between the mTOR and Hippo signaling cascades. However, mechanisms of regulation involving direct crosstalk between the Hippo and mTOR pathways remain unknown.

mTOR forms two functional multiprotein complexes, known as complex 1 (mTORC1) and complex 2 (mTORC2), by interacting with specific adaptor proteins. Raptor and Rictor are the main components of mTORC1 and mTORC2, respectively, and their deletion causes selective disruption of their respective complexes (Laplante and Sabatini, 2012; Wullschleger et al., 2006). Most of what is known about the cellular functions and substrates of mTOR in mammals pertains to mTORC1. On the other hand, there is still little known about the biology of mTORC2. Homozygous systemic deletion of Rictor is embryonically lethal (Guertin et al., 2006; Shiota et al., 2006; Yang et al., 2006), and inducible systemic Rictor disruption reduces lifespan (Lamming et al., 2014), suggesting that mTORC2 is involved in the regulation of important cellular mechanisms and functions in mammals. However, the cellular functions, substrates, and molecular mechanisms regulated by mTORC2 in different tissues and organs still remain to be clarified.

The Hippo pathway is composed of a group of evolutionarily conserved protein kinases that inhibit cellular growth and promote apoptosis (Pan, 2010; Yu and Guan, 2013). The core component of this group of kinases is MST1, which phosphorylates and activates LATS kinases, which in turn phosphorylate and inhibit YAP1, a co-transcription factor that promotes proliferation and survival. The Hippo pathway is inhibited in several different types of cancer cells, whereas it is activated during cellular stress, when it promotes cell-cycle arrest and death (Pan, 2010; Yu and Guan, 2013). The mechanisms through which the Hippo pathway is regulated under both unstressed and stressed conditions are poorly understood.

Tight control over cellular growth and survival appears to be particularly important in the heart, where regulation of cardiac

CrossMark

of cellular survival and growth. Finally, we discovered a mechanism of regulation of the Hippo pathway and a mechanism of direct crosstalk between the mTOR and Hippo pathways.

RESULTS

mTORC2 Is Required for the Maintenance of Cardiac Dimensions and Function as well as Left Ventricular Growth in Response to Pressure Overload

We dissected the role of mTORC2 in the heart using a Cre/loxP strategy to condi-

mass and cardiomyocyte survival is critical for homeostasis and adaptation to stress. The mTOR and Hippo pathways appear to be important regulators of cellular growth and survival in the heart as well. Previous studies demonstrated that mTORC1 promotes cardiac growth and preserves cardiac function in the adult heart through the inhibition of 4E-BP1 protein (Sciarretta et al., 2014; Shende et al., 2011; Tamai et al., 2013; Zhang et al., 2010; Zhu et al., 2013). In contrast, activation of MST1 promotes dilated cardiomyopathy, contributes to cardiomyocyte death during ischemic injury, and inhibits cardiac growth (Del Re et al., 2014; Maejima et al., 2013; Yamamoto et al., 2003). What is still unclear is the importance of mTORC2 in the regulation of cellular growth and survival in the heart, as well as how MST1 activity is controlled in the heart.

In the present study, we show that mTORC2 is a negative regulator of MST1 activity in the heart. We found that mTORC2 preserves cardiac structure and function and compensatory growth in response to mechanical stress by restraining the activity of MST1. Three main aspects of this study establish its relevance. The role of mTORC2 in the regulation of cardiomyocyte survival and size in the heart was elucidated. In addition, MST1 was identified as a substrate of mTORC2 in the regulation

tionally delete the Rictor gene in cardiomyocytes (Shiota et al., 2006). Flox mice carrying a Rictor allele in which exon 3 is flanked by two loxP sites were cross-bred with mice with cardiomyocyte-specific overexpression of Cre recombinase under the control of the α-myosin heavy chain (MHC) promoter. Mice with α-MHC-Cre-mediated homozygous deletion of Rictor (R-cKO mice) displayed a significant reduction in the Rictor protein level in the heart with respect to control mice (Figure 1A). On the other hand, the Raptor protein level was unchanged in R-cKO mice (Figure 1A). R-cKO mice were born alive and developed normally. At 2 months of age, they did not display any difference in cardiac dimensions or function with respect to control mice (Figure S1). However, at 6 months of age, R-cKO mice exhibited significant cardiac dilation and a reduction of systolic function with respect to both control mice and mice with heterozygous Rictor knockout (Figures 1B and 1C). R-cKO mice also showed a significant increase in cardiac fibrosis and apoptosis, as indicated by an increased percentage of TUNEL-positive cells (Figures 1D–1F). These results indicate that mTORC2 is required for the maintenance of cardiac structure and function in the adult heart. Of note, the fact that mice with heterozygous Rictor knockout (Rictor flox/+ and α-MHC-Cre+) did not show

in both R-cKO and control mice, as indicated by increases in left ventricular weight/tibia length. However, the TAC-induced left ventricular hypertrophy was attenuated in R-cKO mice as compared to controls (Figure 2F), suggesting a defect in the hypertrophic response to TAC in R-cKO mice. This result was also confirmed by assessment of the cardiomyocyte cross-sectional area, as evaluated using wheat germ agglutinin staining of left ventricular tissue sections, which showed that the increase in cell size after TAC is modestly but significantly attenuated in R-cKO mice with respect to controls (Figures 3A and 3B). Cardiac apoptosis was also significantly increased in the hearts of R-cKO mice after TAC, whereas fibrosis was similar in control mice (Figures 3C–3F). Pressure overload induced increases in the percentage of Ki-67-positive cardiomyocytes in control mouse hearts. However,

significant cardiac abnormalities excludes the possibility that Cre overexpression alone was responsible for the cardiac phenotype of R-cKO mice.

Next, we subjected young R-cKO mice, which did not show baseline cardiac abnormalities, as described above, to transverse aortic constriction (TAC), an intervention that imposes high blood pressure (pressure overload) on the left ventricle of the heart. After 4 weeks of pressure overload, both longitudinal and transverse sections of the hearts of R-cKO mice showed significant cardiac dilation and wall thinning (Figures 2A and 2B). Echocardiographic analyses also indicated that R-cKO mice show cardiac dilation, wall thinning, and systolic dysfunction as compared to controls after TAC (Figures 2C, 2D, and S2A–S2C). R-cKO mice also showed more severe signs of heart failure after TAC, including a marked increase in lung weight and left ventricular end-diastolic pressure (Figures 2E and S2D). TAC induced significant left ventricular hypertrophy

R-cKO mice displayed a lower percentage of Ki-67-positive cardiomyocytes, suggesting that cardiomyocyte proliferation in response to pressure overload is attenuated in R-cKO mice (Figures 3G and 3H). Overall, these results demonstrate that R-cKO mice develop severe heart failure in response to pressure overload. Although heart failure with cardiac dilation and dysfunction is commonly accompanied by left ventricular hypertrophy in order to reduce wall stress, such a compensatory hypertrophy was attenuated in R-cKO mice. This suggests that endogenous Rictor/mTORC2 plays a significant role in mediating cardiac hypertrophy in response to pressure overload.

Rictor/mTORC2 Disruption Promotes Cardiac Dysfunction and Heart Failure through Deregulated Activation of MST1

We then investigated the molecular mechanisms through which Rictor/mTORC2 regulates survival and growth of

A

B BASELINE   TAC

C

D CT TAC   RICTOR cKO TAC

E

F BASELINE   TAC

G

H DAPI   Ki67 / TnT   MERGED
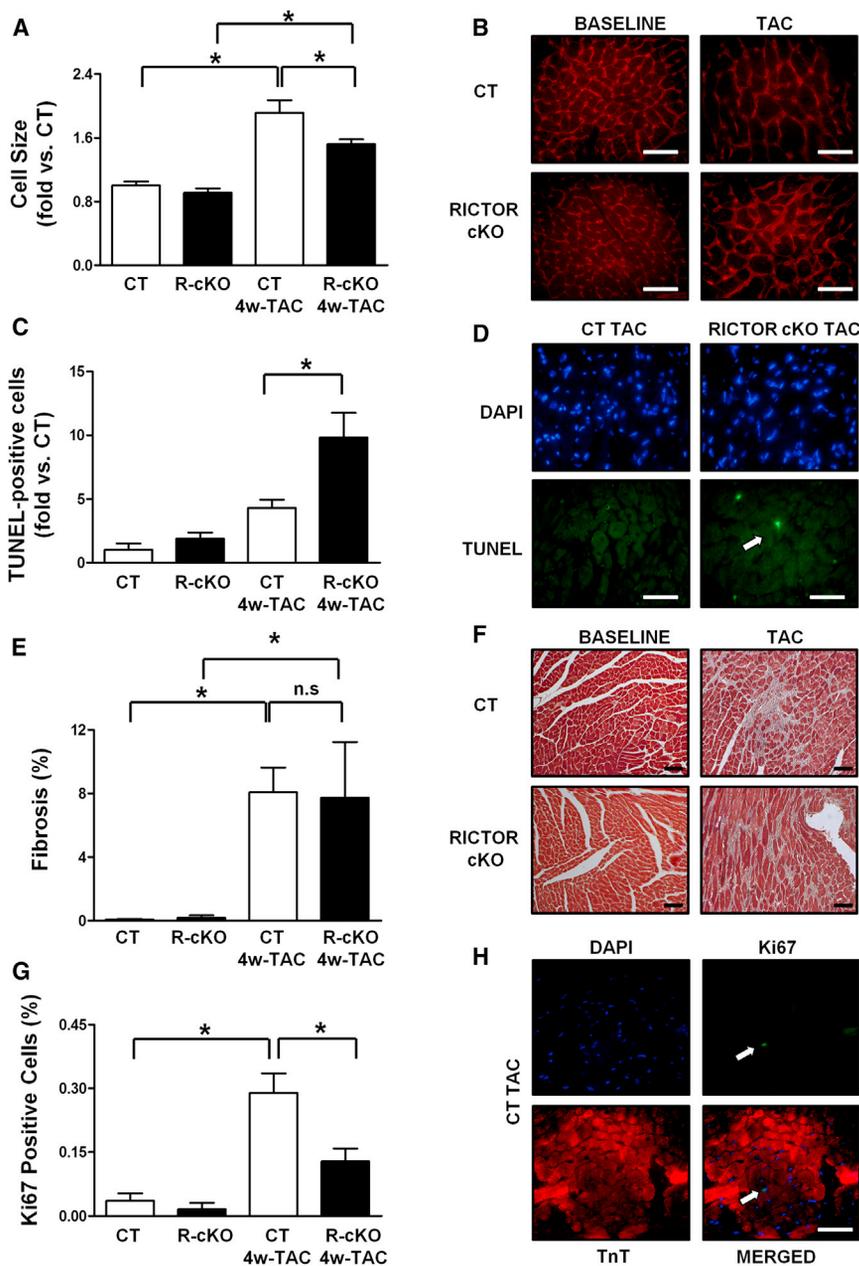
Figure 3. Rictor/mTORC2 Disruption Impairs Left Ventricular Growth and Promotes Apoptosis in Response to Pressure Overload

Wheat germ agglutinin, TUNEL, Masson's trichrome and Ki67 stainings were performed in left ventricular sections from CT and R-cKO mice at baseline and after 4 weeks of pressure overload.

(B, D, F, and H) Representative pictures are shown.

(A, C, E, and G) Cell size (A), percentage of TUNEL-positive cells (C), percentage of fibrosis (E), and percentage of Ki67-positive cells (G) were measured. n = 3–5. n.s., not significant.

All data are expressed as mean ± SEM and as fold versus CT when specified. *$p < 0.05$. Scale bar represents 100 μm.

cardiomyocytes. To this end, we evaluated the potential downstream signaling pathways of mTORC2 in R-cKO and control mice at baseline and after 2 days of TAC, which represents an early phase of pressure overload. This early time point allows for evaluation of the signaling pathways initially modulated in response to TAC before heart failure develops and other pathways are secondarily altered. AKT phosphorylation at serine 473 was significantly increased after TAC with respect to baseline in control mice (Figures S3A and S3C), suggesting that mTORC2 is significantly and rapidly activated in response to pressure overload. As expected, we found that there was significantly less myocardial AKT phosphorylation at serine 473 in R-cKO mice at baseline and after TAC, whereas phosphory-

lation at threonine 308 was unchanged in R-cKO mice (Figures S3A, S3C, and S3D). mTORC1 activity, as evaluated by p70S6 kinase phosphorylation, was also increased after TAC but did not differ between R-cKO and control mice (Figures S3A and S3E). Phosphorylation of GSK-3β at serine 9 and FOXO1 at threonine 24, two main downstream targets of AKT, also did not differ between R-cKO mice and control mice during the early phase of TAC, although the protein level of GSK-3β was increased and FOXO1 phosphorylation was reduced in the hearts of R-cKO mice after 4 weeks of TAC (Figures S3A, S3B, and S3F–S3I).

The myocardial activity of MST1, as evaluated by its autophosphorylation at threonine 183, was significantly increased in R-cKO mice as compared to control mice, both at baseline and after 2 days of TAC (Figures 4A, S4A, and S4B). MST1 phosphorylation remained higher in R-cKO mice even after 4 weeks of TAC (Figures 4B and S4C). In addition, MST1 cleavage, a marker of strong MST1 and caspase activation, was markedly increased in the hearts of R-cKO mice after TAC (Figures 4B and S4D). Phosphorylation of LATS2 and YAP, two major downstream components of the Hippo pathway, was also significantly increased in R-cKO mice with respect to control mice, both at baseline and in response to TAC (Figure S4E). MST1 is a main component of the Hippo pathway, which negatively regulates organ size through stimulation of apoptosis and inhibition of cell proliferation (Del Re et al., 2014; Maejima et al., 2013; Pan, 2010; Yamamoto et al., 2003; Yu and Guan, 2013). We previously demonstrated that cardiac-specific overexpression of MST1 in transgenic mice (Tg-MST1) promotes cardiac dilation and dysfunction associated with cardiac fibrosis, apoptosis, and inhibition of compensatory cardiomyocyte growth (Yamamoto

Figure 4. Rictor/mTORC2 Disruption Promotes Cardiac Dysfunction and Dilation through MST1 Activation

(A and B) Phosphorylated, total and cleaved levels of MST1 were evaluated in the hearts of CT and R-cKO mice at baseline and after pressure overload. Representative immunoblots are shown, and densitometric analyses are shown in Figure S4.

(C) Six-month-old CT, R-cKO, DN-MST1, and R-cKO+DN-MST1 mice underwent echocardiographic analysis. Fractional shortening (FS) was measured. n = 3–7.

(D–F) CT, R-cKO, DN-MST1, and R-cKO+DN-MST1 mice around 10 weeks of age were subjected to 4 weeks of TAC and then underwent echocardiographic analysis. Left ventricular end-diastolic diameter (LVEDD), fractional shortening (FS), and lung weight/tibia length (TL) were measured. n = 3–7.

All data are expressed as mean ± SEM. *p < 0.05.

ously found to inhibit MST1 (Collak et al., 2012). Rictor knockdown in cardiomyocytes in vitro was associated with a marked activation of MST1 that could not be rescued by concomitant overexpression of constitutively active AKT (Figure S5). This result suggests that mTORC2 may regulate MST1 in cardiomyocytes independently of AKT. In addition, previous studies demonstrated that AKT1 knockout mice do not show any baseline cardiac abnormalities, whereas they develop a marked increase in cardiac hypertrophy with respect to control mice after TAC (DeBosch et al., 2006), which is different from the phenotype of R-cKO mice that show attenuated left ventricular hypertrophy after TAC. Therefore, we tested the hypothesis that mTORC2 can directly regulate MST1 activity. Rictor and MST1 were partially co-localized in cardiomyocytes, mainly in the perinuclear region, which is consistent with the previously reported localization of Rictor and MST1 in the ER (Boulbés et al., 2011; Maejima et al., 2013) (Figure 5A). In addition, we found that endogenous Rictor interacts with MST1 in the mouse heart in vivo and in cardiomyocytes in vitro (Figures 5B and S6A).

Next, we evaluated whether mTORC2 can phosphorylate MST1. Since mTORC2 is a multiprotein complex composed of several proteins that are required for its activity, in order to test whether mTORC2 can phosphorylate specific substrates, we needed to purify mTORC2 from a biological system by immunoprecipitating Rictor, incubating it with a specific substrate, and performing in vitro kinase assays (Sarbassov et al., 2005). We used kinase-dead MST1 as a substrate to avoid the strong MST1 autophosphorylation that is usually observed when wild-type MST1 is used in kinase assays (Maejima et al., 2013). Phosphorylation of MST1 by mTORC2 was unaffected by an AKT inhibitor but was abrogated by Torin1, an mTOR-specific

et al., 2003). The cardiac phenotype of Tg-MST1 was remarkably similar to that observed in R-cKO mice after TAC. We therefore hypothesized that R-cKO mice develop cardiac dysfunction and dilation through deregulated activation of MST1 kinase. In order to test this hypothesis, we cross-bred R-cKO mice with mice overexpressing dominant-negative MST1 (kinase-dead MST1) in a cardiomyocyte-specific manner (Yamamoto et al., 2003). MST1 inhibition by dominant-negative MST1 almost completely rescued the cardiac dysfunction observed in 6-month-old R-cKO mice at baseline (Figure 4C). In addition, we found that MST1 inhibition significantly rescued cardiac dysfunction and heart failure in young R-cKO mice after 4 weeks of TAC (Figures 4D–4F). This result indicates that Rictor/mTORC2 disruption promotes cardiomyopathy and heart failure through MST1 activation.

Rictor/mTORC2 Phosphorylates MST1 in the SARAH Domain, Thereby Reducing Its Dimerization and Activity

mTORC2 may regulate MST1 activity either directly or indirectly through the modulation of AKT activity. In fact, AKT was previ-

Figure 5. Rictor/mTORC2 Phosphorylates MST1 at Serine 438

(A) Immunocytofluorescence assay of Rictor and MST1 was performed in neonatal rat cardiomyocytes transduced with either control adenovirus or an adenovirus expressing a short-hairpin sequence targeting Rictor or MST1. Representative pictures are shown. A higher magnification of a portion of the merged panel of control sample is shown in the inset. Scale bar represents 50 μm.

(B) Rictor was immunoprecipitated from mouse left ventricle. Immunoprecipitate with control IgG was used as control. Representative immunoblots of Rictor and MST1 are shown.

inhibitor (Thoreen et al., 2009) (Figure 5C). These results suggest that mTORC2 phosphorylates MST1 through an mTOR-dependent but AKT-independent mechanism. In order to identify the MST1 phosphorylation site, mass spectrometry analysis was conducted on recombinant MST1 phosphorylated by mTORC2. The result of the mass spectrometry analysis indicated that mTORC2 phosphorylates MST1 at serine 438 (Figure 5D). This residue of MST1 is evolutionarily conserved across different species, although serine may be substituted with threonine in non-mammalian species (Figure 5E). Serine 438 is located in the SARAH domain of MST1 (Figure 5F), which is highly conserved from lower organisms to mammals and is of crucial importance for MST1 dimerization, autophosphorylation and subsequent activation (Praskova et al., 2004).

Using an antibody that is specific against MST1 phosphorylated at serine 438 (Figures S6B–S6D), we confirmed that mTORC2 phosphorylates MST1 at serine 438, after mTORC2 kinase reaction using recombinant MST1 as a substrate (Figure 5G). We also found that phosphorylation of MST1 at this site is significantly reduced in the hearts of R-cKO mice (Figures 5H and S4F) and in cardiomyocytes with Rictor depletion in vitro (Figure S5). On the other hand, phosphorylation of MST1 at serine 438 was significantly increased in response to TAC, suggesting that MST1 phosphorylation by mTORC2 is increased during cardiac stress (Figures 5H and S4F). Interestingly, we found that insulin, a known activator of mTORC2 (Lamming et al., 2012; Xie et al., 2011) and cellular growth, induces MST1 phosphorylation at serine 438 in cardiac fibroblasts. In contrast, mTOR inhibition by Torin1 significantly inhibited serine 438 phosphorylation and induced a marked increase in MST1 autophosphorylation (Figure S6E). These results suggest that mTORC2 also regulates and phosphorylates MST1 in other cell types as well as in cardiomyocytes and that serine 438 phosphorylation negatively regulates MST1 activation.

Given that MST1 was dramatically activated and autophosphorylated in R-cKO mice, we hypothesized that MST1 phosphorylation at serine 438 by endogenous mTORC2 may interfere with the dimerization and activation of MST1. To test this hypothesis, wild-type, serine 438 phosphorylation-resistant mutant and serine 438 phosphorylation-mimicking mutant MST1, with either MYC or FLAG tags, were expressed in cells in different combinations, and co-immunoprecipitation assays were conducted. The dimeric interaction between phosphomimetic MST1 mutant (S438D) and wild-type MST1 was significantly less than that between two wild-type MST1 proteins or between phosphoresistant MST1 mutant (S438A) and wild-type MST1 (Figure 6A). These results indicate that phosphorylation of MST1 at serine 438 interferes with MST1 dimerization.

Overexpression of either wild-type or S438A MST1 was able to significantly increase the phosphorylation of the downstream target LATS2 in cardiomyocytes. In contrast, S438D MST1 failed to induce significant phosphorylation of LATS2 (Figures 6B and 6C). Finally, overexpression of either wild-type or S438A MST1 significantly reduced cardiomyocyte survival. On the other hand, overexpression of S438D MST1 in cardiomyocytes failed to induce significant cell death (Figure 6D). Overall, these results indicate that mTORC2-dependent phosphorylation of MST1 at serine 438 inhibits MST1 homodimerization and activity, as well as MST1-induced cell death.

DISCUSSION

The mTOR kinase is a master regulator of cellular growth and survival (Laplante and Sabatini, 2012; Wullschleger et al., 2006). However, the cellular processes and downstream signaling pathways specifically regulated by mTORC2 still remain to be clarified. Here, we demonstrate the existence of a direct connection between mTORC2 and the Hippo pathway. Disruption of mTORC2 leads to deregulated activation of MST1 that causes cardiomyocyte apoptosis and cardiac dysfunction while, at the same time, suppressing compensatory myocardial growth. Thus, our study provides evidence indicating that mTORC2 promotes cellular growth and survival by restraining MST1 activity. In addition, we clarified a direct signaling link between the mTOR and Hippo pathways that is crucial for the preservation of cardiac function and growth in response to stress.

mTORC2 phosphorylates MST1 at serine 438 in the SARAH domain and reduces its ability to homodimerize and become activated. The SARAH domain is a highly conserved module located in the C-terminal portion of MST1 that is necessary for homodimerization (Praskova et al., 2004). The SARAH domain is also involved in heterodimerization with other SARAH-domain-containing scaffolds, including RASSF1A, NORE1, and SAV1, that regulate MST1 activity as well (Pan, 2010; Praskova et al., 2004; Yu and Guan, 2013). A previous crystallographic analysis of the MST1 SARAH domain homodimer indicated that serine 438 is located between helix h1 and helix h2 and, together with tryptophan 439, it forms a bifurcated hydrogen bond with phenylalanine 435 (Hwang et al., 2007). This bifurcated hydrogen bond formation plays an important role in stabilizing the kinked conformation of helix h1 against helix h2, which in turn facilitates the autophosphorylation of the kinase domain of MST1. We speculate that phosphorylation of serine 438 may disturb the kinked conformation of the helix h1/h2, thereby interfering with both MST1 homodimerization and autophosphorylation. In addition, the crystallographic structure of the homodimer

(C) Kinase reaction was performed with the specified proteins. 50 μM of 1L-6-hydroxymethyl-chiro-inositol2-[(R)-2-O-methyl-3-O-octadecylcarbonate] or 1 μM of Torin1 was used when specified. A representative autoradiograph is shown. A portion of the samples used in each kinase reaction was used for immunoblot analysis to test the levels of FLAG-DN-MST1, Rictor, and mTOR.

(D) Analysis of the MST1 peptide by tandem mass spectrometry after incubation with the mTORC2 complex in a kinase reaction.

(E) Conservation of MST1 serine 438 across different species is shown.

(F) Schema representing the localization of the serine 438 residue in the MST1 SARAH domain.

(G) A kinase reaction was performed with recombinant MST1 in the presence or absence of mTORC2. Torin1 was used when specified. After the kinase reaction, MST1 phosphorylation at serine 438 was evaluated.

(H) Cardiac phosphorylation levels of MST1 at serine 438 were evaluated in CT and R-cKO at baseline and after TAC. Immunoblots are shown.
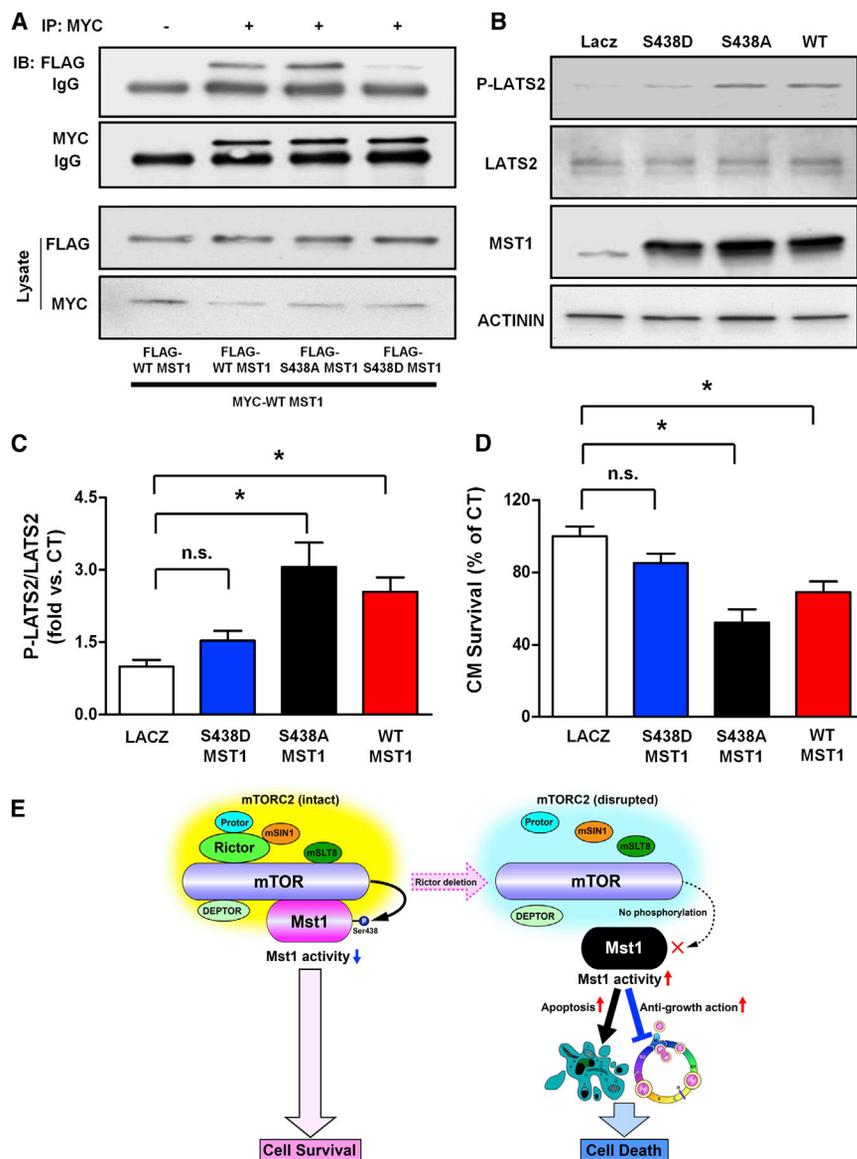
Figure 6. MST1 Phosphorylation at Serine 438 Reduces Its Dimerization and Activity

(A) COS7 cells were transfected with the specified plasmids. MYC was immunoprecipitated, and immunoblots for MYC and FLAG are shown. Immunoprecipitate with control IgG was used as a control.

(B and C) Cardiomyocytes were transduced with ad-LacZ, ad-FLAG-WT-MST1, ad-FLAG-S438A-MST1, or ad-FLAG-S438D-MST1. After 48 hr, the levels of phospho-LATS2 (T1041 homologous), total LATS2, and MST1 were evaluated, and representative immunoblots are shown (B) together with quantification analysis of the P-LATS2/LATS2 ratio (C). n = 3.

(D) After 72 hr, cardiomyocyte survival was assessed by CellTiter-Blue assay. n = 4. All data are expressed as mean ± SEM. *p < 0.05; n.s., not significant.

(E) Schema representing the negative regulation of MST1 by mTORC2, which preserves cell survival.

regard, we observed that MST1 activity is increased in the hearts of wild-type mice during pressure overload. MST1 is activated under this condition through several upstream molecules, such as RASSF1a and KRAS, which were previously found to mediate MST1 activation during cardiac stress (Del Re et al., 2010, 2014). However, we found that mTORC2-dependent phosphorylation of MST1 is also increased during pressure overload and that when mTORC2 is disrupted, MST1 activity further increases and cardiac dysfunction occurs. This suggests that the activity of mTORC2 toward MST1 is increased under this condition in order to maintain MST1 activation within physiological limits and preserve cardiac function. Other molecules also appear to have similar functions,

of MST1 SARAH domains (Hwang et al., 2007) also suggests that serine 438 on one molecule of MST1 is located close to the aspartate 475 and glutamate 478 residues located on the other molecule of MST1. Thus, phosphorylation of serine 438 would interfere with the dimerization of MST1 through electrostatic repulsion (Figure S6F). Finally, as already mentioned, it is also possible that phosphorylation of serine 438 would modulate the ability of MST1 to hetero-dimerize with RASSF/SAV1 proteins.

Previous studies indicated that, at physiological levels, Hippo signaling controls cellular growth and maintains organ structure, whereas deregulated Hippo signaling activation during stress is maladaptive and causes apoptosis and cell death (Pan, 2010; Yu and Guan, 2013). We believe that an important function of mTORC2 is to be a "guardian" of MST1 activity, finely controlling when MST1 activation is physiological or detrimental. In this

acting to keep the level of activity of MST1 low. For example, NORE1 was shown to restrain MST1 activity in vivo (Praskova et al., 2004). In addition, previous work indicated that RAF1 protein inhibits apoptosis and promotes cell survival by preventing the dimerization and activation of MST2 (O'Neill et al., 2004). Our study significantly extends this evidence and demonstrates that phosphorylation of MST1 by mTORC2 is another mechanism for limiting MST1 activity. Of note, this inhibitory mechanism appears to be specific for MST1, since the other MST isoform, MST2, lacks the serine 438 site in its primary structure. In addition, recent evidence indicates that MST2 exerts pro-hypertrophic effects in cardiomyocytes and does not regulate cardiac function in response to pressure overload (Zi et al., 2014). This diverges from the known anti-hypertrophic and pro-heart-failure effects of MST1 in the heart and from the cardiac effects of mTORC2 disruption, as we demonstrated in our study. This prior

evidence coupled with our results suggest that the detrimental effects of mTORC2 disruption are mediated by MST1 activation, whereas MST2 is likely not involved but warrants further study.

mTORC2 positively regulates cellular growth and survival, mainly through the positive regulation of AKT (Jacinto et al., 2006; Jacinto et al., 2004; Sarbassov et al., 2005). The mTORC2/AKT pathway was also found to be associated with cardiomyocyte protection during ischemic injury (Völkers et al., 2013; Yano et al., 2014). We believe that our study significantly expands upon this evidence by demonstrating that mTORC2 is also able to regulate cellular growth and survival in specific cell types and conditions through the direct inhibition of MST1. Of note, previous evidence from Guan's laboratory indicated that YAP, a main target of inhibition by the Hippo pathway, can activate AKT through miR-29-mediated inhibition of PTEN (Tumaneng et al., 2012). These data, combined with our results, indicate that mTORC2 can regulate AKT activity both directly and indirectly through the inhibition of the Hippo pathway and the resulting activation of YAP. In addition, AKT and MST1 were previously shown to mutually inhibit each other (Cinar et al., 2011; Collak et al., 2012). Thus, the mTORC2 and Hippo pathways can engage in crosstalk at multiple levels. Of note, mTORC2 was also shown to activate SGK1 and PRKCA/PKC-α (Facchinetti et al., 2008; García-Martínez and Alessi, 2008; Ikenoue et al., 2008). However, it is very unlikely that these factors are involved in the detrimental effects of mTORC2 deletion in the heart, since inhibition of either SGK1 or PKC-α protects the heart against hemodynamic stress (Braz et al., 2004; Das et al., 2012).

We believe that the molecular mechanisms presented in our study have broad biological implications. mTORC2 was previously shown to positively regulate survival of cancer cells (Laplante and Sabatini, 2012). On the other hand, the components of the Hippo pathway are onco-suppressors that are inhibited in different types of cancer (Pan, 2010). Our study suggests that mTORC2 may regulate carcinogenesis through the inhibition of Hippo signaling. In this regard, recent work reporting the results of a large-scale proteomics analysis of the human kinome conducted in leukemia, colon, and breast cancer cell lines showed that MST1 is phosphorylated at serine 438 in all of these cancer cell lines, whereas MST1 autophosphorylation could not be detected, indicating MST1 inhibition (Oppermann et al., 2009). These results are consistent with our evidence indicating that phospho-serine 438 inhibits MST1 activity. Notably, mTORC2 was shown to mediate survival of leukemia, colon, and breast cancer cell lines (Laplante and Sabatini, 2012; Wullschleger et al., 2006).

Another potential and relevant implication of the connection between mTORC2 and the Hippo pathway relates to the control of cytoskeleton organization. mTORC2 was previously shown to promote actin polymerization and F-actin accumulation, through which it regulates cell migration and proliferation (Jacinto et al., 2004). On the other hand, the components of the Hippo pathway exhibit opposite effects on cytoskeleton organization, inhibiting actin polymerization and F-actin accumulation (Fernández et al., 2011). Our results suggest that mTORC2 may also promote actin formation indirectly through inhibition of the Hippo pathway. F-actin accumulation induced by mTORC2 may also

represent an indirect mechanism of regulation of the Hippo pathway by mTORC2, since actin polymerization results in Hippo signaling inhibition and YAP1 activation (Aragona et al., 2013; Zhao et al., 2012).

Our data may also be relevant to completely different biological systems and organisms. For example, amphibians are among the organisms with the highest regenerative capacity. The frog *Xenopus laevis* was shown to be able to regenerate amputated limbs through the activation of YAP, suggesting Hippo pathway inhibition (Hayashi et al., 2014). Of note, in the MST1 homolog in *X. laevis*, serine 438 is substituted with aspartic acid, suggesting a lower MST1 activity, which is consistent with an increased regenerative ability.

In conclusion, our study demonstrates the existence of crosstalk between the mTORC2 and Hippo pathways. We believe that the mTORC2/MST1 signaling cascade is a critical regulator of cell survival and growth in cardiomyocytes and, potentially, in other biological systems (Figure 6E).

EXPERIMENTAL PROCEDURES

Animal Models

The generation of *Rictor* flox mice was previously described (Shiota et al., 2006). Rictor exon 3 was targeted in these animals. Flox mice were cross-bred with α-MHC-Cre transgenic mice in order to generate R-cKO mice. α-MHC-DN-MST1 (K59R) transgenic mice (C57BL/6J background) were previously described (Yamamoto et al., 2003). R-cKO mice were cross-bred with Tg-DN-MST1 mice. All mice were studied on a C57BL/6J background. Control (CT), R-cKO, and R-cKO+DN-MST1 mice were subjected to TAC to induce pressure overload, as previously described (Yamamoto et al., 2003). Briefly, mice were anesthetized with pentobarbital sodium. The left chest was opened and mice were ventilated. Aortic constriction was performed by ligation of the transverse thoracic aorta with a 26G needle using a 7-0 braided polyester suture. Echocardiographic and hemodynamic analyses were performed as previously described (Maejima et al., 2013; Yamamoto et al., 2003). All protocols concerning animal use were approved by the institutional animal care and use committee at Rutgers New Jersey Medical School.

Cell Cultures, Plasmid Constructs, Transfection, and Adenovirus Generation

Primary cultures of ventricular cardiomyocytes were prepared from 1-day-old Crl:(WI) BR Wistar rats (Charles River Laboratories) as described previously (Maejima et al., 2013). Percoll gradient centrifugation was performed to separate the cardiomyocyte fraction from other cellular fractions. Cells were cultured in DMEM/F-12 medium. HEK293 cells and COS7 cells were maintained as previously described (Maejima et al., 2013). Neonatal rat cardiac fibroblasts were isolated, passaged, and maintained as previously described (Del Re et al., 2010). MYC-Rictor expression construct was from Addgene (Sarbassov et al., 2004). WT-MST1, AKT1, S438A-MST1, and S438D-MST1 cDNAs were subcloned into pDC316 vector (Maejima et al., 2013; Morisco et al., 2001; Yamamoto et al., 2003). Lipofectamine 2000 (Invitrogen) was used for transfection. Adenovirus vector generation was conducted as described previously (Yamamoto et al., 2003). The ΔE1 adenoviral genome incorporated in pBHGloxΔE1,3Cre (Microbix) was co-transfected with the pDC316 shuttle vector harboring the cDNA of interest into HEK293 cells.

Immunoprecipitation and Immunoblot Analysis

Left ventricular tissue homogenates or cell cultures were lysed with CHAPS buffer (40 mM HEPES [pH 7.5], 120 mM NaCl, 1 mM EDTA, 0.3% CHAPS) for mTORC2 immunoprecipitation or with IGEPAL CA-630 buffer (50 mM Tris-HCl [pH 7.4], 1% IGEPAL CA-630, 10 mM EDTA, 150 mM NaCl), together with a protease inhibitor cocktail (Sigma-Aldrich). For FLAG-DN-MST1

immunoprecipitation, cells were lysed with a buffer containing 50 mM Tris-HCl (pH 7.5), 300 mM NaCl, 1% Triton X-100, 0.5% deoxycholic acid, 1 mM EDTA, and protease inhibitors.

Lysates were incubated with the specified antibody and the immunocomplexes were precipitated using A/G Sepharose beads for at least 2 hr at 4°C. After immunoprecipitation, the samples were washed five times and were used for in vitro kinase assay reactions or for immunoblotting after immunoprecipitate elution.

Immunoblot analysis was performed as previously described (Maejima et al., 2013). For this analysis, tissue or cellular samples were lysed in RIPA buffer with 0.1 mM Na$_3$VO$_4$, 1 mM NaF, 1 mM β-glycerophosphate, and protease inhibitor cocktail from Sigma-Aldrich.

In Vitro Kinase Assay

MYC-Rictor was immunoprecipitated from HEK293 cells to isolate mTORC2 as described previously (Dibble et al., 2009; Sarbassov et al., 2004; Treins et al., 2010). mTORC2 was incubated with purified FLAG-DN-MST1 in the presence of mTORC2 kinase buffer (25 mM HEPES [pH 7.4], 100 mM potassium acetate, and 1 mM MgCl$_2$), together with 500 μM of ATP, with or without 10 μCi [γ-^{32}P] ATP per reaction for 20 min at 37°C, as previously described (Dibble et al., 2009; Ikenoue et al., 2009; Sarbassov et al., 2006; Sarbassov et al., 2005). The AKT inhibitor 1L-6-hydroxymethyl-chiro-inositol2-[(R)-2-O-methyl-3-O-octadecylcarbonate] (Biovision, Cat# 1701-1) or Torin1 (Tocris, Cat# 4247) was used when specified. Phosphorylated proteins were separated by SDS-PAGE and analyzed by autoradiography.

Mass Spectrometry

After kinase reaction with recombinant MST1 protein (1 μg), the samples were separated by SDS-PAGE and the MST1 band was excised for in-gel trypsin digestion. The resulting peptides were subjected to liquid chromatography-tandem mass spectrometry analysis on the Orbitrap Velos tandem mass spectrometry instrument (Thermo Scientific) using a nanoelectrospray source with a spray voltage of 2 kV. Mass spectrometry (MS) spectra were acquired in a positive ion mode. MS/MS spectra were acquired using collision-induced dissociation (CID) in a data-dependent manner. The lock mass was used for accurate mass measurements. The MS/MS spectra were searched against Swiss-Prot human database using the Mascot search engine. The following search parameters were used: trypsin was selected as the enzyme with 1 missed cleavage; peptide precursor mass tolerance of 10 ppm; and MS/MS mass tolerance of 0.5 Da. Methionine oxidation, serine and threonine phosphorylation, and cysteine carbamidomethylation were selected as variable modifications. The phosphopeptides and their phosphorylation sites were verified with PhosphoRS software (Thermo Scientific).

Immunofluorescence and Staining

Cellular and tissue immunofluorescence were conducted according to a previously described method (Maejima et al., 2013). Briefly, neonatal rat cardiomyocytes plated on chamber slides (Lab-Tek) were fixed with 4% paraformaldehyde and permeabilized with PBS containing 0.1% Triton X-100. Mouse left ventricles were fixed in formalin and sectioned at 10-μm thickness. Tissue sections were then subjected to deparaffinization and antigen unmasking using citrate buffer and washed with PBS containing 0.3% Triton X-100. Samples were then blocked for 1 hr with PBS containing 5% BSA in vitro experiments or with normal goat serum in vivo, and then incubated with primary antibody overnight. Cells were then incubated with Alexa 488- and Alexa Fluor 568-conjugated secondary antibodies (Invitrogen) for 3 hr. Nuclei were stained with DAPI. Images were taken using either conventional or confocal microscopy. For TUNEL staining, we used the In Situ Cell Death Detection kit (Roche) according to the manufacturer's instructions. Masson's trichrome, H&E, and wheat germ agglutinin staining were conducted as previously described (Del Re et al., 2013; Maejima et al., 2013).

Cell Survival Assay

Cardiomyocyte survival was assessed using the CellTiter-Blue assay from Promega, according to the manufacturer's instructions.

Antibodies

Polyclonal antibody against MST1 phosphorylated at serine 438 was raised in rabbits and generated by 21st Century Biochemicals. The immunizing peptides were GDYEFLK[pS]WTVEDL and DYEFLK[pS]WTVEDLQ. Phospho-LATS2 (Thr1041) was kindly provided by Dr. Nojima (Osaka University). Other commercially available antibodies used in the study include Rictor, MST1 (P-Thr183), MST1 (N terminus), Raptor, AKT1 (P-Ser473), AKT1 (P-Thr308), AKT1, p70S6K (P-Thr389), GSK-3β (P-Ser9), GSK-3β, FOXO1 (P-Thr32/24), FOXO1, YAP1 (Ser127), YAP1, GAPDH, anti-mouse, anti-rabbit, conformation-specific anti-rabbit, and FLAG from Cell Signaling; MST1 (C terminus) from BD Transduction; p70S6K and Rictor from Santa Cruz Biotechnology; FLAG, FLAG-agarose beads, MYC, and Tubulin from Sigma-Aldrich; Rictor and LATS2 from Bethyl Laboratories; Ki-67 from Vector Laboratories; Troponin T from Neomarkers; and Alexa 488 donkey anti-goat immunoglobulin G (IgG), Alexa 488 goat anti-rabbit IgG, Alexa Fluor 594 goat anti-mouse IgG, and Alexa Fluor 568 donkey anti-mouse IgG from Invitrogen.

Statistics

Data are expressed as mean ± SEM. The t test was used when the difference in means between two groups was evaluated. One-way ANOVA followed by the Bonferroni post hoc test was used when the comparison analysis was extended to multiple groups. Statistical analyses were performed with the use of GraphPad-Prism 5.00 (GraphPad-Software). p values of < 0.05 were considered statistically significant.

SUPPLEMENTAL INFORMATION

Supplemental Information includes six figures and can be found with this article online at http://dx.doi.org/10.1016/j.celrep.2015.03.010.

AUTHOR CONTRIBUTIONS

ACKNOWLEDGMENTS

REFERENCES

Aragona, M., Panciera, T., Manfrin, A., Giulitti, S., Michielin, F., Elvassore, N., Dupont, S., and Piccolo, S. (2013). A mechanical checkpoint controls multicellular growth through YAP/TAZ regulation by actin-processing factors. Cell 154, 1047–1059.

Boulbés, D.R., Shaiken, T., and Sarbassov, D. (2011). Endoplasmic reticulum is a main localization site of mTORC2. Biochem. Biophys. Res. Commun. 413, 46–52.

Braz, J.C., Gregory, K., Pathak, A., Zhao, W., Sahin, B., Klevitsky, R., Kimball, T.F., Lorenz, J.N., Nairn, A.C., Liggett, S.B., et al. (2004). PKC-alpha regulates cardiac contractility and propensity toward heart failure. Nat. Med. *10*, 248–254.

Cinar, B., Collak, F.K., Lopez, D., Akgul, S., Mukhopadhyay, N.K., Kilicarslan, M., Gioeli, D.G., and Freeman, M.R. (2011). MST1 is a multifunctional caspase-independent inhibitor of androgenic signaling. Cancer Res. *71*, 4303–4313.

Collak, F.K., Yagiz, K., Luthringer, D.J., Erkaya, B., and Cinar, B. (2012). Threonine-120 phosphorylation regulated by phosphoinositide-3-kinase/Akt and mammalian target of rapamycin pathway signaling limits the antitumor activity of mammalian sterile 20-like kinase 1. J. Biol. Chem. *287*, 23698–23709.

Das, S., Aiba, T., Rosenberg, M., Hessler, K., Xiao, C., Quintero, P.A., Ottaviano, F.G., Knight, A.C., Graham, E.L., Boström, P., et al. (2012). Pathological role of serum- and glucocorticoid-regulated kinase 1 in adverse ventricular remodeling. Circulation *126*, 2208–2219.

DeBosch, B., Treskov, I., Lupu, T.S., Weinheimer, C., Kovacs, A., Courtois, M., and Muslin, A.J. (2006). Akt1 is required for physiological cardiac growth. Circulation *113*, 2097–2104.

Del Re, D.P., Matsuda, T., Zhai, P., Gao, S., Clark, G.J., Van Der Weyden, L., and Sadoshima, J. (2010). Proapoptotic Rassf1A/Mst1 signaling in cardiac fibroblasts is protective against pressure overload in mice. J. Clin. Invest. *120*, 3555–3567.

Del Re, D.P., Yang, Y., Nakano, N., Cho, J., Zhai, P., Yamamoto, T., Zhang, N., Yabuta, N., Nojima, H., Pan, D., and Sadoshima, J. (2013). Yes-associated protein isoform 1 (Yap1) promotes cardiomyocyte survival and growth to protect against myocardial ischemic injury. J. Biol. Chem. *288*, 3977–3988.

Del Re, D.P., Matsuda, T., Zhai, P., Maejima, Y., Jain, M.R., Liu, T., Li, H., Hsu, C.P., and Sadoshima, J. (2014). Mst1 promotes cardiac myocyte apoptosis through phosphorylation and inhibition of Bcl-xL. Mol. Cell *54*, 639–650.

Dibble, C.C., Asara, J.M., and Manning, B.D. (2009). Characterization of Rictor phosphorylation sites reveals direct regulation of mTOR complex 2 by S6K1. Mol. Cell. Biol. *29*, 5657–5670.

Facchinetti, V., Ouyang, W., Wei, H., Soto, N., Lazorchak, A., Gould, C., Lowry, C., Newton, A.C., Mao, Y., Miao, R.Q., et al. (2008). The mammalian target of rapamycin complex 2 controls folding and stability of Akt and protein kinase C. EMBO J. *27*, 1932–1943.

Fernández, B.G., Gaspar, P., Brás-Pereira, C., Jezowska, B., Rebelo, S.R., and Janody, F. (2011). Actin-Capping Protein and the Hippo pathway regulate F-actin and tissue growth in Drosophila. Development *138*, 2337–2346.

García-Martínez, J.M., and Alessi, D.R. (2008). mTOR complex 2 (mTORC2) controls hydrophobic motif phosphorylation and activation of serum- and glucocorticoid-induced protein kinase 1 (SGK1). Biochem. J. *416*, 375–385.

Guertin, D.A., Stevens, D.M., Thoreen, C.C., Burds, A.A., Kalaany, N.Y., Moffat, J., Brown, M., Fitzgerald, K.J., and Sabatini, D.M. (2006). Ablation in mice of the mTORC components raptor, rictor, or mLST8 reveals that mTORC2 is required for signaling to Akt-FOXO and PKCalpha, but not S6K1. Dev. Cell *11*, 859–871.

Hayashi, S., Tamura, K., and Yokoyama, H. (2014). Yap1, transcription regulator in the Hippo signaling pathway, is required for Xenopus limb bud regeneration. Dev. Biol. *388*, 57–67.

Hwang, E., Ryu, K.S., Pääkkönen, K., Güntert, P., Cheong, H.K., Lim, D.S., Lee, J.O., Jeon, Y.H., and Cheong, C. (2007). Structural insight into dimeric interaction of the SARAH domains from Mst1 and RASSF family proteins in the apoptosis pathway. Proc. Natl. Acad. Sci. USA *104*, 9236–9241.

Ikenoue, T., Inoki, K., Yang, Q., Zhou, X., and Guan, K.L. (2008). Essential function of TORC2 in PKC and Akt turn motif phosphorylation, maturation and signalling. EMBO J. *27*, 1919–1931.

Ikenoue, T., Hong, S., and Inoki, K. (2009). Monitoring mammalian target of rapamycin (mTOR) activity. Methods Enzymol. *452*, 165–180.

Jacinto, E., Loewith, R., Schmidt, A., Lin, S., Rüegg, M.A., Hall, A., and Hall, M.N. (2004). Mammalian TOR complex 2 controls the actin cytoskeleton and is rapamycin insensitive. Nat. Cell Biol. *6*, 1122–1128.

Jacinto, E., Facchinetti, V., Liu, D., Soto, N., Wei, S., Jung, S.Y., Huang, Q., Qin, J., and Su, B. (2006). SIN1/MIP1 maintains rictor-mTOR complex integrity and regulates Akt phosphorylation and substrate specificity. Cell *127*, 125–137.

Lamming, D.W., Ye, L., Katajisto, P., Goncalves, M.D., Saitoh, M., Stevens, D.M., Davis, J.G., Salmon, A.B., Richardson, A., Ahima, R.S., et al. (2012). Rapamycin-induced insulin resistance is mediated by mTORC2 loss and uncoupled from longevity. Science *335*, 1638–1643.

Lamming, D.W., Mihaylova, M.M., Katajisto, P., Baar, E.L., Yilmaz, O.H., Hutchins, A., Gultekin, Y., Gaither, R., and Sabatini, D.M. (2014). Depletion of Rictor, an essential protein component of mTORC2, decreases male lifespan. Aging Cell *13*, 911–917.

Laplante, M., and Sabatini, D.M. (2012). mTOR signaling in growth control and disease. Cell *149*, 274–293.

Maejima, Y., Kyoi, S., Zhai, P., Liu, T., Li, H., Ivessa, A., Sciarretta, S., Del Re, D.P., Zablocki, D.K., Hsu, C.P., et al. (2013). Mst1 inhibits autophagy by promoting the interaction between Beclin1 and Bcl-2. Nat. Med. *19*, 1478–1488.

Morisco, C., Seta, K., Hardt, S.E., Lee, Y., Vatner, S.F., and Sadoshima, J. (2001). Glycogen synthase kinase 3beta regulates GATA4 in cardiac myocytes. J. Biol. Chem. *276*, 28586–28597.

O'Neill, E., Rushworth, L., Baccarini, M., and Kolch, W. (2004). Role of the kinase MST2 in suppression of apoptosis by the proto-oncogene product Raf-1. Science *306*, 2267–2270.

Oppermann, F.S., Gnad, F., Olsen, J.V., Hornberger, R., Greff, Z., Kéri, G., Mann, M., and Daub, H. (2009). Large-scale proteomics analysis of the human kinome. Mol. Cell. Proteomics *8*, 1751–1764.

Pan, D. (2010). The hippo signaling pathway in development and cancer. Dev. Cell *19*, 491–505.

Praskova, M., Khoklatchev, A., Ortiz-Vega, S., and Avruch, J. (2004). Regulation of the MST1 kinase by autophosphorylation, by the growth inhibitory proteins, RASSF1 and NORE1, and by Ras. Biochem. J. *381*, 453–462.

Sarbassov, D.D., Ali, S.M., Kim, D.H., Guertin, D.A., Latek, R.R., Erdjument-Bromage, H., Tempst, P., and Sabatini, D.M. (2004). Rictor, a novel binding partner of mTOR, defines a rapamycin-insensitive and raptor-independent pathway that regulates the cytoskeleton. Curr. Biol. *14*, 1296–1302.

Sarbassov, D.D., Guertin, D.A., Ali, S.M., and Sabatini, D.M. (2005). Phosphorylation and regulation of Akt/PKB by the rictor-mTOR complex. Science *307*, 1098–1101.

Sarbassov, D.D., Ali, S.M., Sengupta, S., Sheen, J.H., Hsu, P.P., Bagley, A.F., Markhard, A.L., and Sabatini, D.M. (2006). Prolonged rapamycin treatment inhibits mTORC2 assembly and Akt/PKB. Mol. Cell *22*, 159–168.

Sciarretta, S., Volpe, M., and Sadoshima, J. (2014). Mammalian target of rapamycin signaling in cardiac physiology and disease. Circ. Res. *114*, 549–564.

Shende, P., Plaisance, I., Morandi, C., Pellieux, C., Berthonneche, C., Zorzato, F., Krishnan, J., Lerch, R., Hall, M.N., Rüegg, M.A., et al. (2011). Cardiac raptor ablation impairs adaptive hypertrophy, alters metabolic gene expression, and causes heart failure in mice. Circulation *123*, 1073–1082.

Shiota, C., Woo, J.T., Lindner, J., Shelton, K.D., and Magnuson, M.A. (2006). Multiallelic disruption of the rictor gene in mice reveals that mTOR complex 2 is essential for fetal growth and viability. Dev. Cell *11*, 583–589.

Tamai, T., Yamaguchi, O., Hikoso, S., Takeda, T., Taneike, M., Oka, T., Oyabu, J., Murakawa, T., Nakayama, H., Uno, Y., et al. (2013). Rheb (Ras homologue enriched in brain)-dependent mammalian target of rapamycin complex 1 (mTORC1) activation becomes indispensable for cardiac hypertrophic growth after early postnatal period. J. Biol. Chem. *288*, 10176–10187.

Thoreen, C.C., Kang, S.A., Chang, J.W., Liu, Q., Zhang, J., Gao, Y., Reichling, L.J., Sim, T., Sabatini, D.M., and Gray, N.S. (2009). An ATP-competitive mammalian target of rapamycin inhibitor reveals rapamycin-resistant functions of mTORC1. J. Biol. Chem. *284*, 8023–8032.

Treins, C., Warne, P.H., Magnuson, M.A., Pende, M., and Downward, J. (2010). Rictor is a novel target of p70 S6 kinase-1. Oncogene *29*, 1003–1016.

Tumaneng, K., Schlegelmilch, K., Russell, R.C., Yimlamai, D., Basnet, H., Mahadevan, N., Fitamant, J., Bardeesy, N., Camargo, F.D., and Guan, K.L. (2012). YAP mediates crosstalk between the Hippo and PI(3)K–TOR pathways by suppressing PTEN via miR-29. Nat. Cell Biol. *14*, 1322–1329.

Völkers, M., Konstandin, M.H., Doroudgar, S., Toko, H., Quijada, P., Din, S., Joyo, A., Ornelas, L., Samse, K., Thuerauf, D.J., et al. (2013). Mechanistic target of rapamycin complex 2 protects the heart from ischemic damage. Circulation *128*, 2132–2144.

Wullschleger, S., Loewith, R., and Hall, M.N. (2006). TOR signaling in growth and metabolism. Cell *124*, 471–484.

Xie, X., Zhang, D., Zhao, B., Lu, M.K., You, M., Condorelli, G., Wang, C.Y., and Guan, K.L. (2011). IkappaB kinase epsilon and TANK-binding kinase 1 activate AKT by direct phosphorylation. Proc. Natl. Acad. Sci. USA *108*, 6474–6479.

Yamamoto, S., Yang, G., Zablocki, D., Liu, J., Hong, C., Kim, S.J., Soler, S., Odashima, M., Thaisz, J., Yehia, G., et al. (2003). Activation of Mst1 causes dilated cardiomyopathy by stimulating apoptosis without compensatory ventricular myocyte hypertrophy. J. Clin. Invest. *111*, 1463–1474.

Yang, Q., Inoki, K., Ikenoue, T., and Guan, K.L. (2006). Identification of Sin1 as an essential TORC2 component required for complex formation and kinase activity. Genes Dev. *20*, 2820–2832.

Yano, T., Ferlito, M., Aponte, A., Kuno, A., Miura, T., Murphy, E., and Steenbergen, C. (2014). Pivotal role of mTORC2 and involvement of ribosomal protein S6 in cardioprotective signaling. Circ. Res. *114*, 1268–1280.

Yu, F.X., and Guan, K.L. (2013). The Hippo pathway: regulators and regulations. Genes Dev. *27*, 355–371.

Zhang, D., Contu, R., Latronico, M.V., Zhang, J., Rizzi, R., Catalucci, D., Miyamoto, S., Huang, K., Ceci, M., Gu, Y., et al. (2010). MTORC1 regulates cardiac function and myocyte survival through 4E-BP1 inhibition in mice. J. Clin. Invest. *120*, 2805–2816.

Zhao, B., Li, L., Wang, L., Wang, C.Y., Yu, J., and Guan, K.L. (2012). Cell detachment activates the Hippo pathway via cytoskeleton reorganization to induce anoikis. Genes Dev. *26*, 54–68.

Zhu, Y., Pires, K.M., Whitehead, K.J., Olsen, C.D., Wayment, B., Zhang, Y.C., Bugger, H., Ilkun, O., Litwin, S.E., Thomas, G., et al. (2013). Mechanistic target of rapamycin (Mtor) is essential for murine embryonic heart development and growth. PLoS ONE *8*, e54221.

Zi, M., Maqsood, A., Prehar, S., Mohamed, T.M., Abou-Leisa, R., Robertson, A., Cartwright, E.J., Ray, S.G., Oh, S., Lim, D.S., et al. (2014). The mammalian Ste20-like kinase 2 (Mst2) modulates stress-induced cardiac hypertrophy. J. Biol. Chem. *289*, 24275–24288.